Results in Physics 16 (2020) 102921

Contents lists available at ScienceDirect

Results in Physics

journal homepage: www.elsevier.com/locate/rinp

Acoustical hooks: A new subwavelength self-bending beam

Constanza Rubio[a,*], Daniel Tarrazó-Serrano[a], Oleg V. Minin[b,c], Antonio Uris[a], Igor V. Minin[b,c]

[a] Centro de Tecnologías Físicas: Acústica, Materiales y Astrofísica, Universitat Politècnica de València, Camino de Vera s/n, 46022 Valencia, Spain
[b] Tomsk Polytechnic University, 36 Lenin Avenue, Tomsk 634050, Russia
[c] Tomsk State University, 30 Lenin Avenue, Tomsk 634050, Russia

ARTICLE INFO

Keywords:
Ultrasound focusing
Acoustic bending beam
Near field focusing

ABSTRACT

In this work, we report the first experimental observation of a new type of near-field curved acoustic beam confirmed by simulations. This new curved acoustical beam is generated by asymmetric distribution of the vortices in a polymer Janus particle (particle with broken symmetry) immersed in water. The origin of the vortices is in the conversion of an incident longitudinal wave mode to a shear wave in a solid and then back to a longitudinal wave in the water and has unique features, the radius of curvature of acoustical hook is less than the wavelength. Indeed, it is the smallest radius of curvature ever recorded for any acoustical beams. These results may be potentially useful when an object, located in the path of the beam, must be avoided. It could also have potential applications in particle manipulations.

Introduction

It is well known since antiquity that waves propagate in a straight line. However, the possibility of a wave propagating along a curved path was suggested and observed experimentally in optics in 2007 [1,2]. The concept arises from quantum mechanics in which, in the absence of an external force, a wave packet can be accelerated as long as the quantum wave function follows an Airy function profile [3]. The exact solution of the Schrödinger equation and the paraxial optical wave equation gives rise to a beam that accelerates in a certain trajectory, that is to say it bends, and being free diffraction. This type of beam was called an Airy beam. It could be noted that the main lobe of a finite energy Airy beam is not observable directly behind the cubic phase element and a transition region exists, where the initial intensity distribution of the incoming beam is transformed into the distinct Airy pattern [4]. Since then, curved beams in optics have attracted great attention from researchers and possible applications have been proposed. In a recent Review paper, Efremidis et al. [5] provided an overview of fundamental findings, developments and applications in the field of accelerating waves.

On the other hand, recently, a new family of near-field localized curved optical beams has been discovered by Minin and Minin [6], which differs from the family of Airy beams. This new family is able to form in the near-field zone the so-called "photonic hook", which is self-bending (transversely accelerate) throughout propagation in near field in free space [7]. Unlike the Airy-like beam, the photonic hook is created by focusing a plane wave through a dielectric particle combination of a wedge prism and a cuboid, and because of this shape with broken symmetry, the time of the full oscillation phase of an optical wave varies in a particle unevenly. As a result, a curved light beam is produced at the exit from the particle (near it shadow surface). Photonic hook are unique in that their radius of curvature is substantially smaller than the wavelength [7,8]. That is, such structured light beams have the maximum acceleration among the known curvilinear beams - the curvature of electromagnetic waves with such a small radius were described for the first time in Refs. [6,7] and confirmed experimentally in this year 2019, by Minin and Minin and colleagues in Terahertz range [8]. The phenomenon of photonic hook was demonstrated also for surface plasmon wave [9] realized in the in-plane of the interface despite the strong energy dissipation at metal surface. These results have generated expectation in the scientific community [10].

Not long ago, and by using the formal analogy between electromagnetic and acoustic waves, Minin and Minin [11] transferred the idea of photonic jet effect [12] to acoustic waves. They demonstrated the existence of the phenomenon of the phononic jet in the shadow area of a penetrable sphere, which they called "acoustojet" (AJ) [13]. For the experimental demonstration of the AJ phenomenon, a Rexolite® sphere with a diameter of 8 wavelengths immersed in water and at a frequency of 1.01 MHz was used [14]. Rexolite® was chosen so that there would not be a significant difference between the impedance of the material and that of the surrounding medium, since otherwise the intensity of the acoustic jet would be relatively low [15].

* Corresponding author.
E-mail address: crubiom@fis.upv.es (C. Rubio).

https://doi.org/10.1016/j.rinp.2019.102921
Received 25 November 2019; Received in revised form 30 December 2019; Accepted 30 December 2019
Available online 07 January 2020

Taking into account this formal analogy between electromagnetic and acoustic waves [11] it can be expected that the photonic hook formation method [7] can be adapted to acoustics. However, unlike electromagnetic waves, where three parameters are decisive: particle shape, refractive index contrast, and particle size, in acoustics, due to the different nature of the waves, five parameters are already determining - the shape of the particle, the contrast of the speed of sound in the medium and the particle, the size of the particle and the contrast of the density of the material of the medium and particle, and for solids, the transverse (shear) speed of sound. This fact causes them to become anisotropic. Therefore, the possibility of implementing the effect of the acoustic hook is not so obvious. So, to this day, not an experiment was ever reported on acoustic hook (AH) effect in liquids. Here, we are going to introduce a simple method to generate the acoustic hook, which can be used to bend, as desired, the acoustic beam in near field without sophisticated control-devices. Its simplicity would make the fabrication process easier and less expensive.

In this work, we show both by simulations and experimentally that a rectangular trapezoidal Rexolite® particle on which a plane ultrasonic wave impinges can generate a curved acoustic beam with unique properties, with radius of curvature substantially smaller than the wavelength in water. In addition, the influence of the inner angle of the rectilinear trapezoid in the generation of the curved beam is analyzed numerically.

Numerical modelling and experimental set-up

The results of the simulation were obtained using the commercial software COMSOL Multiphysics Modeling © and with 3D modeling. Two resolution modules have been used with the perfectly coupled multiphysics solution system to be able to consider the two propagation speeds (longitudinal and shear speed) in the rectangular trapezoidal particle of Rexolite®. The type of mesh was adjusted to free tetrahedral, and to avoid numerical dispersion, the maximum size of the element was $\lambda/8$.

The host medium was water with typical sound speed (c) and density (ρ) values ($c_{water} = 1500$ m·s^{-1} and $\rho_{water} = 1000$ kg·m^{-3}). The working frequency selected for the simulations was 250 kHz. The values used to model Rexolite® were longitudinal sound speed $c_{lRexolite} = 2337$ m·s^{-1}, shear sound speed $c_{sRexolite} = 1157$ m·s^{-1}, and density $\rho_{Rexolite} = 1049$ kg·m^{-3} [28–30].

The experimental measurements were carried out by using the technique of ultrasonic immersion transmission. A precision automated measurement system was used. This system consists of a fixed-piston ultrasonic transducer used as an emitter (Imasonic, Les Savourots, France) with a central frequency of 250 kHz and an active diameter of 0.032 m and, as a receiver, a polyvinylidene fluoride needle hydrophone (PVDF) (model HPM1 / 1, acoustic precision Ltd., Dorchester, United Kingdom) with a diameter of 1.5 mm ($\lambda/6$, where λ is the incident wavelength in water) and a bandwidth of ± 4 dB spanning from 200 kHz to 15 MHz. To post-amplify and digitize the signal was used a digital oscilloscope for PC (model 3224 of Picoscope, Pico Technology, St. Neots, United Kingdom). The scanning was carried out with steps of 1 mm and during the measurements; the water temperature was 18 °C. The experimental set-up is shown in Fig. 1(a)-(b).

To demonstrate experimentally the phenomenon of AH generation, a cuboid and a rectangular trapezoidal particle were machined from a cylinder using a numerical control milling machine. Rexolite® was chosen as material to manufacture the samples. Rexolite® is a plastic cross-linked polystyrene that has low difference in acoustic impedance with respect to water. The cuboid has equal side length, l. The value of side length chosen was 3λ ($\lambda = 6$ mm). The rectangular trapezoidal sample is obtained from the 3λ side cuboid and had an interior angle of 20°, as shown in Fig. 1(c).

Results

Fig. 2 shows the simulation results obtained to describe the normalized sound pressure $\frac{|P|^2}{|P_i|^2}$ distributions (where p is the pressure at each point and p_i is the incident sound pressure) in XZ planes for Rexolite® cuboid particle and rectangular trapezoidal particles with different interior angles. As can be seen in Fig. 2(a), an acoustic field enhancement appears on the shadow surface of the cuboid particle. This phenomenon is the AJ. When the cuboid is replaced by a rectangular trapezoid with an interior angle of 10°, it is observed that the shape of the AJ is slightly bent (see Fig. 2(b)). As the interior angle increases, taking values of 15° (Fig. 2(c)) and 20° (Fig. 2(d)), it is observed that the curvature of the AJ increases. For interior angles values higher than 20°, it is observed that the effect weakens (Fig. 2(e)-(f)). To quantify how much the AJ is bent, the curvature is defined. As defined in Refs. 24–25, the AJ curvature is determined by a midline L_{jet} aided by an angle β between the two lines, which link the start point with the inflection point and the inflection point with the end point, respectively, see Fig. 3. Table 1 summarizes the AJ curvature as a function of rectangular trapezoid interior angle α. As can be observed, the cuboid particle, that has symmetry ($\alpha = 0°$), produces a symmetric AJ, that is, without curvature ($\beta = 0°$). When the symmetry of the particle is broken using a rectangular trapezoid, the AJ ceases to be symmetrical and begins to bend. As the interior angle α increases, the angle of curvature β increases, it should be note that for an angle α of 30° the effect is no longer perceptible.

Interestingly, in the case of acoustic hook, only main lobe has a curved shape and the family of curved side lobes, as in Airy beams are absent. The pressure maximum not located on the shadow surface of the particle, as is the case in optics, and shifted to a distance of about 0.17λ from the surface of the particle. The minimal FWHM of AJ for cube is located at the shadow surface of cube and is about 1.7λ. In the case of a particle with broken symmetry minimal FWHM of AH is 0.717λ at the shadow surface of particle (i.e. has a subwavelength value) and FWHM is about 0.83λ at the point of maximal pressure along AH.

The technique of ultrasonic immersion was used to experimentally verify the self-bending effect of an AJ. A cuboid particle of side length 3λ, and a rectangular trapezoidal particle obtained from the 3λ side cuboid and with an interior angle of 20° were chosen (see Fig. 3(a)-(c)). The experimental results for the cuboid particle and the rectangular trapezoidal particle are shown in Fig. 4(a) and (b) respectively. Fig. 4(b) clearly shows the effect of the formation of a curvilinear region of the acoustic field localization behind a dielectric particle with broken symmetry. It could be observed that an experimental curvature $\beta = 36°$ is obtained. It must be kept in mind that the simulations carried out and shown in Fig. 2(a)-(f) have been carried out considering the incidence of a plane wave. However, the emission of the transducer is not really plane wave, although the particles were at a relatively long distance from the transducer. However, the experimental results agree well with the simulated results, which allow validate the results of the simulations presented in this work.

Table 2 shows the parameters of the experimental acoustic hook for the rectangular trapezoidal particle. It is observed that the lateral dimensions (FWHM/λ) of the AH are subwavelength and improves the experimental results obtained in the AJ: for the cross-section III, which corresponds to $Z/\lambda = 0.667$, an FWHM/$\lambda = 1.169$ is obtained of the cuboid particle, while in the case of the rectangular trapezoidal particle an FWHM/$\lambda = 0.557$ is obtained. Thus, the phenomenon of AH could provide advantages over the AJ in certain applications since it improves the spatial resolution.

The AH phenomenon can be explained by using the relative intensity ($\vec{I} = p\hat{A}\cdot\vec{u}$, where p is the acoustic pressure and $\vec{u}$ is the particle velocity) flow diagrams in XZ planes for the particles considered. Fig. 5(a) shows the relative flow diagrams in XZ plane for the 3λ side cuboid particle. It is observed that there are regions within the cuboid

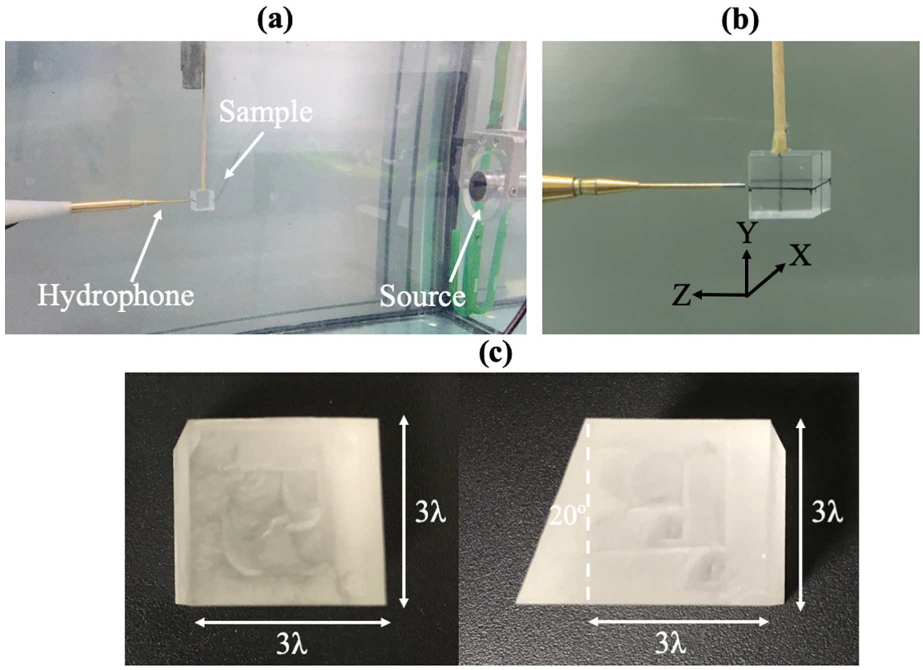

Fig. 1. Detail of (a) experimental set-up, (b) coordinate axes. (a) Rexolite® particles considered.

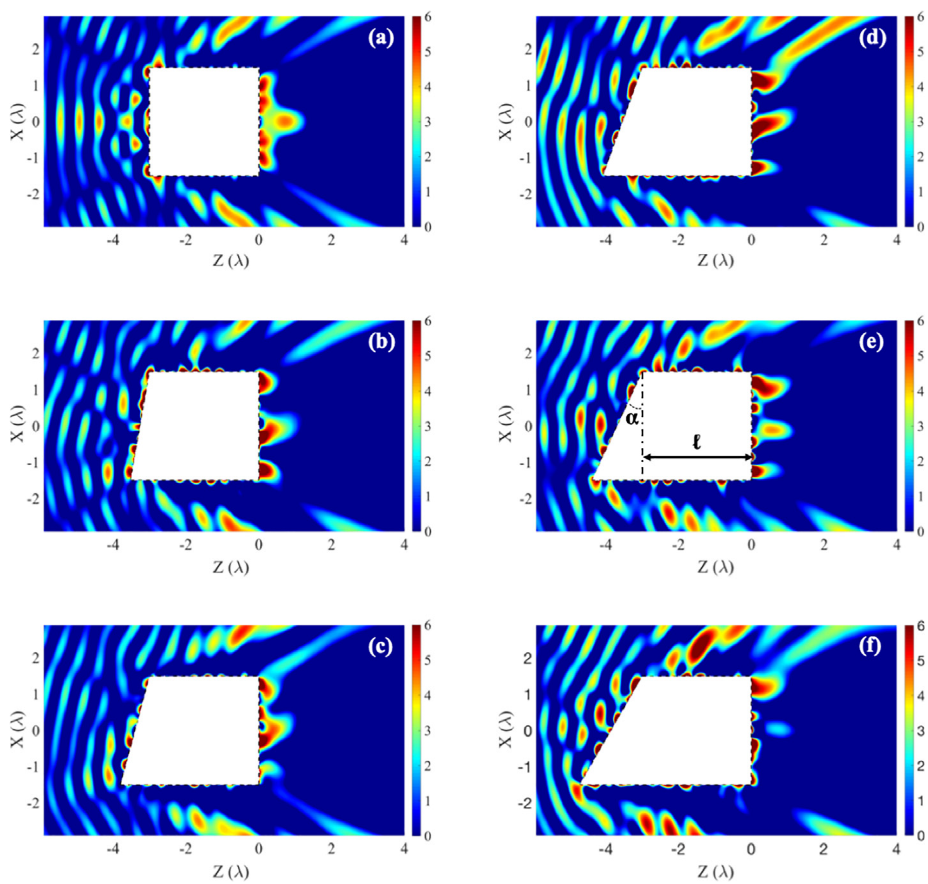

Fig. 2. Normalized sound pressure $\frac{|p|^2}{|p_i|^2}$ distributions in XZ planes for different Rexolite® particles: (a) 3λ side cuboid, and a rectangular trapezoidal particle obtained from the 3λ side cuboid and with an interior angle (b) 10°, (c) 15°, (d) 20°, (e) 25° and (f) 30°.

where the intensity lines produce vortices that redirect the intensity flow to different areas of the cuboid [7,8]. Due to the cuboid's symmetry, the distribution of the vortices is symmetrical, so that the AJ obtained is completely symmetrical, that is, it is not curved. However, when the rectangular trapezoidal particle is considered (see Fig. 5(b)), it is observed that the distribution of the vortices that redirect the

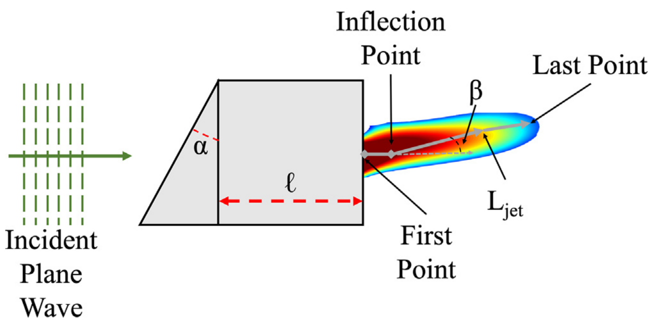

Fig. 3. Scheme of the curved beam formation.

Table 1
Curvatures β of AH for different interior angle α.

α	0°	10°	15°	20°	25°	30°
β	0°	12°	30°	38°	46°	–

intensity flow inside the particle is no longer symmetric. This produces the curvature of the AJ. The origin of the vortices is in the conversion of an incident longitudinal wave mode to a shear wave in a solid and then back to a longitudinal wave in the water. The particle velocity fields, $\vec{v}$, can be represented by gradients of the scalar function ϕ in a fluid [15]

$$\vec{v} = \vec{\nabla}\phi$$

and the curl of a vector field $\vec{\Psi}$ in a solid

$$\vec{v} = \vec{\nabla}\phi + \vec{\nabla} \times \vec{\Psi}$$

where $\vec{\nabla}\phi$ represents the longitudinal wave and $\vec{\nabla} \times \vec{\Psi}$ represents the shear wave.

Table 2
Parameters of the experimental acoustic hook in different cross-sections.

Cross-section	Z/λ	FWHM/λ
I	0.333	0.707
II	0.500	0.825
III	0.667	0.557
IV	0.833	0.707
V	1.000	1.061

The vortices in the intensity flow are due to shear waves ($\vec{\nabla} \times \vec{\Psi} \neq 0$). In the case of the cuboid particle, there is symmetry in the position of the vortices, while in the case of the rectangular trapezoidal particle, there is no such symmetry, which causes the AJ bent.

The nature of the formation of an AJ and AH consists in the constructive interference of waves passing through a particle and diffracting on its surface (enveloping the particle). Therefore, longitudinal and shear waves create a pressure distribution inside the particle, near its shadow surface, which is a kind of boundary conditions for the wave propagating through the background medium (water). In other words, if we completely exclude the dielectric particle from consideration, and we take the pressure distribution on its shadow surface as the boundary conditions of an effective source of acoustic waves, then the effect of the AH also will be observed.

Conclusions

In this wok, it was shown that AH phenomenon is observed near the shadow surface of polymer Janus particle on a scale much smaller than known Airy-family beams.

The intensity flow analysis particles suggests that the origin of the

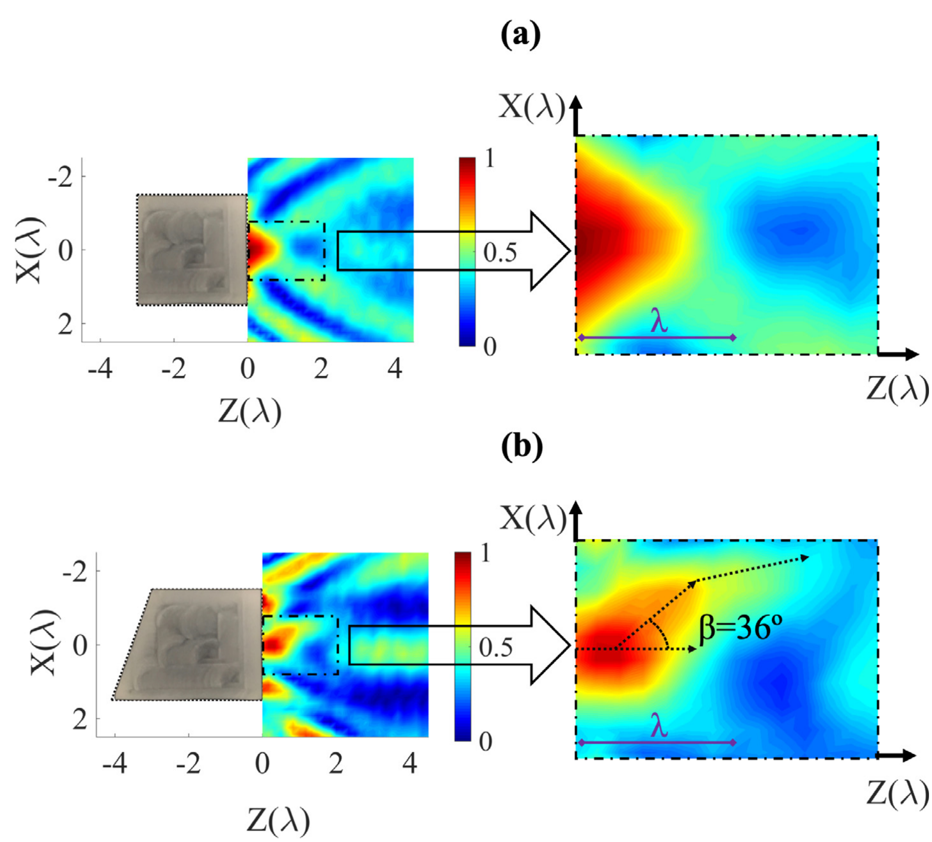

Fig. 4. Measured sound pressure distribution in XZ planes for Rexolite® particles (a) 3λ side cuboid and (b) rectangular trapezoidal particle obtained from the 3λ side cuboid and with an interior angle of 20°.

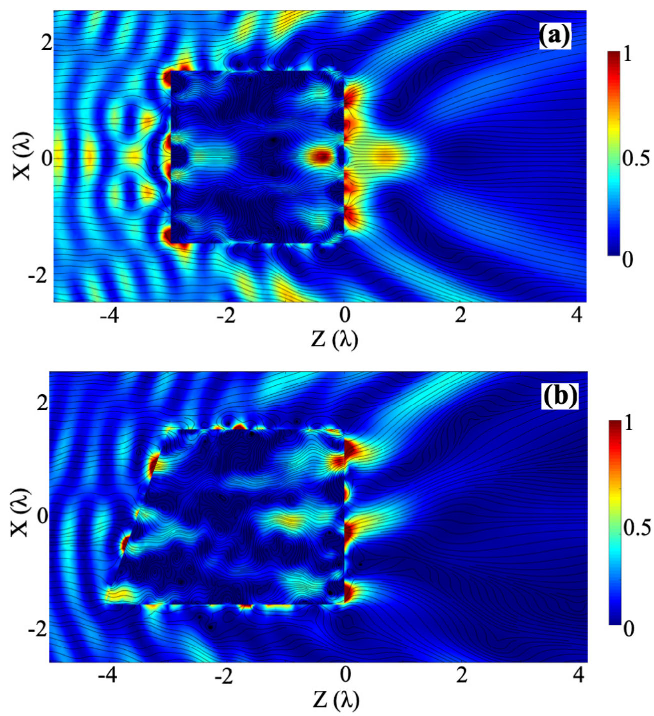

Fig. 5. Numerical normalized relative intensity flow in XZ planes for (a) 3λ side cuboid and (b) rectangular trapezoidal particle obtained from the 3λ side cuboid and with an interior angle of 20°.

AJ bent phenomenon is the vortices that appear inside the particles due to the conversion of the incident longitudinal wave mode to a shear wave in a solid. When the particle is symmetric these vortices are distributed symmetrically, so that the beam does not curve, whereas when the particle is asymmetric, the distribution of the vortices inside the particle no longer symmetrical causing the AJ bending.

The AH as its optical counterpart has unique features of self-bending with radius of curvature that are substantially smaller than the wavelength and represents the smallest radius of curvature ever recorded for any acoustical beams. The AH have the potential to focus around obstacles that are directly in the beam path similar to optical [16,17]. The mesoscale dimensions and simplicity of the AH are much more controllable for practical tasks and could enable it to be integrated, for example, into lab-on-a-chip platforms and indicating their large-scale potential applications.

Thus, we demonstrated an effective design for the generation of ultrasonic self-bending AH through a dielectric Janus particle with broken symmetry, immersed in water. The design route was well demonstrated by full-wave simulations and validated preliminarily by experiments. To our opinion, such elegant examples of structured acoustical beams make possible a deeper understanding of wave propagation, and will fuel anticipation and excitement for the next generation of imaging and near-field manipulation.

Therefore, it has been shown that the concept of photonic hook has gone beyond optics [6,7] and plasmonics [9] and now penetrated acoustics.

Declaration of competing interest

The authors declare that they have no known competing financial interests or personal relationships that could have appeared to influence the work reported in this paper.

CRediT authorship contribution statement

Constanza Rubio: Conceptualization, Software, Investigation, Formal analysis, Writing - original draft, Writing - review & editing, Supervision, Project administration. **Daniel Tarrazó-Serrano:** Software, Investigation, Formal analysis, Visualization, Writing - original draft, Writing - review & editing. **Oleg V. Minin:** Conceptualization, Investigation, Formal analysis, Supervision, Writing - original draft, Writing - review & editing. **Antonio Uris:** Conceptualization, Investigation, Formal analysis, Writing - original draft, Writing - review & editing. **Igor V. Minin:** Conceptualization, Investigation, Formal analysis, Supervision, Writing - original draft, Writing - review & editing.

Acknowledgements

This work has been supported by Spanish Ministry of Science, Innovation and Universities (grant No. RTI2018-100792-B-I00). The research was partially supported by the Russian Foundation for Basic Research (Grant No. 20-57-S52001) and by Tomsk Polytechnic University Competitiveness Enhancement Program. D.T.-S. acknowledges financial support from MICINN BES-2016-07713 project.

References

[1] Siviloglou GA, Broky J, Dogariu A, Christodoulides DN. Observation of accelerating Airy beams. Phys Rev Lett 2007;99:213901.
[2] Siviloglou GA, Christodoulides DN. Accelerating finite energy Airy beams. Opt Lett 2007;32:979.
[3] Berry MV, Balazs NL. Nonspreading wave packets. Am J Phys 1979;47:264.
[4] Valdmann A, Piksarv P, Valtna-Lukner H, Saari P. White-light hyperbolic Airy beams. J Opt 2018;20:095605.
[5] Efremidis NK, Chen Z, Segev M, Christodoulides DN. Airy beams and accelerating waves: an overview of recent advances. Optica 2019;6(5):686–701.
[6] Minin IV, Minin OV. Diffractive Optics and Nanophotonics: Resolution below the Diffraction Limit. Springer; 2016.
[7] Yue L, Minin OV, Wang Z, Monks J, Shalin A, Minin IV. Photonic hook: A new curved light beam. Opt Lett 2018;43(4):771–4.
[8] Minin IV, Minin OV, Katyba GM, Chernomyrdin NV, Kurlov VN, Zaytsev KI, et al. Experimental observation of a photonic hook. Appl Phys Lett 2019;114:031105.
[9] Minin IV, Minin OV, Ponomarev DS, Glinskiy IA. Photonic hook plasmons: a new curved surface wave. Ann Phys 2018;530(12):1800359.
[10] Dholakia K, Bruce GD. Optical hooks. Nat Photonics 2019;13:229–30.
[11] Minin OV, Minin IV. Acoustic analogue of photonic jet phenomenon based on penetrable 3D particle. Opt Quant Electron 2017;49:54.
[12] Luk'yanchuk BS, Paniagua-Domínguez R, Minin IV, Minin OV, Wang Z. Refractive index less than two: photonic nanojets yesterday, today and tomorrow. Opt. Mater. Express 2017;7:1820–47.
[13] Lopes JH, Leão-Neto JP, Minin IV, Minin OV, Silva GT. A theoretical analysis of jets. 22nd Int. Cong. Ac. (ICA 2016), Buenos Aires. 2016.
[14] Lopes JH, Andrade MAB, Leao-Neto JP, Adamowski JC, Minin IV, Silva GT. Focusing acoustic beams with a ball-shaped lens beyond the diffraction limit. Phys Rev Appl 2017;8:024013.
[15] Cremer L, Heckl M. Structure-Borne Sound. 2nd ed.New York: Springer-Verlag; 1988. p. 138.
[16] Minin IV, Minin OV, "Device for forming the optical trap in the form of the photonic hook," Patent of Russia 161207 (27 October, 2015).
[17] Ang AS, Karabchevsky A, Minin IV, Minin OV, Sukhov SV, Shalin AS. 'Photonic Hook' based optomechanical nanoparticle manipulator. Sci Rep 2018;8:2029.